THE LOMA PRIETA, CALIFORNIA, EARTHQUAKE OF OCTOBER 17, 1989:
EARTHQUAKE OCCURRENCE

AFTERSHOCKS AND POSTSEISMIC EFFECTS

A SHEAR STRAIN ANOMALY FOLLOWING THE LOMA PRIETA EARTHQUAKE

By M.T. Gladwin, R.L. Gwyther, and R.H.G. Hart,
University of Queensland, Australia

CONTENTS

ABSTRACT

Borehole tensor strain instruments deployed along the San Andreas fault for the past 10 years have provided sufficient resolution and stability to sample regional tectonic processes. Data obtained from an instrument at San Juan Bautista in the near field region of the Loma Prieta earthquake provide the first high-resolution continuous shear strain observations associated with a large earthquake. A change in fault-parallel shear-strain rate of approximately 1 με per year occurred about a year prior to the earthquake and persisted to the time of the event. The strain rate decreased immediately after the earthquake, but following the Chittenden sequence of earthquakes in April 1989, a new and higher rate of fault-parallel shear accumulation (0.84 με per year relative to the 1989 rate) was established. This strain rate has continued through 1993. Associated creep-rate changes are apparent at a number of sites on the surface trace of the fault within 30 km, indicating that the measured change of strain rate at the time of the earthquake has regional significance. We propose that the observed strain accumulation results from increased slip around a nearby locked section of the fault arising from loading by the failed Loma Prieta source region to the north. This model is consistent with suggestions of an increased probability of a moderate earthquake near San Juan Bautista and with evidence that interactions between fault regions are important in earthquake processes.

INTRODUCTION

A Gladwin borehole tensor strainmeter (Gladwin, 1984) installed near the San Andreas fault at San Juan Bautista in late 1983 has provided continuous areal and shear strain data with sub-nanostrain resolution and long-term stability better than 100 $n\varepsilon$ per year (Gladwin and others, 1987). Raw data from the instrument consist of diameter changes in three directions at 120° to each other in the horizontal plane. These are reduced to areal strain ε_a, and engineering shear strains γ_1 and γ_2 (approximately parallel to and at 45° to the fault respectively), which are defined in terms of strain tensor components (ε_{xx}, ε_{yy} , and ε_{xy} by

$$e_a=\varepsilon_{xx}+\varepsilon_{yy}$$

$$\gamma_1=\varepsilon_{xx}-\varepsilon_{yy}$$

$$\gamma_2=2\varepsilon_{xy}$$

where, as subscripts to ε, the x direction is east and y is north. The strainmeter is grouted into the surrounding rock, and this instrument inclusion is softer to shear than to compression. Observed strain components are thus scaled by hole-coupling parameters (Gladwin and Hart, 1985) determined by tidal calibration.

Data from borehole inclusions are initially dominated by grout compression of the instrument, by thermally controlled decay as the instrument site re-establishes equilibrium with its surroundings, and by an exponential recovery of the virgin stress field relieved at the borehole during the drilling process (Berry and Fairhurst, 1966; Berry, 1967). The exponential signals are characteristic of viscoelastic rheology as typified by Burghers solids (Jaeger and Cook, 1976). They have no relevance to the monitoring of regional strain changes and were removed by an exponential least-squares fitting procedure over the interval January 1984 to February 1988 (Gladwin and others, 1991).

Raw data from the three instrument gauges commencing in 1984 (3 months after installation) are shown in figure 1*A*. In determination of the exponentials to be removed from the raw gauge data streams, all data known to be contaminated were eliminated from the fit (Gladwin and others, 1991; Gwyther and others, 1992). The same intervals of data are used for determination of exponentials for all three gauges, and no linear trend has been removed. The resulting exponentials, determined from data during early 1984, and from May 1986 to April 1988, are shown also in figure 1*A* (offset for clarity). The data following the Morgan Hill earthquake in April 1984 and anomalous data associated with field experiments at the site in 1986 were excluded. The instrument was off line for 6 months during 1987. All data after April 1988 were also excluded and provide no constraint on the least-squares fitting. Figure 1*B* gives the residuals from the determined exponentials. The residuals indicate stable gauge behavior from mid-1986, an emerging anomaly on all components beginning in late 1988, the strain offsets for the Loma Prieta earthquake in October 1989 and significantly differing behavior on all gauges since that time. The postseismic data indicate immediate postseismic recovery for about 3 months, and following the Chittenden earthquakes in April 1990 the establishment of new, relatively linear trends.

These residuals were then reduced to the strains ε_a, γ_1, and γ_2 shown in figure 2*A*. The data differ slightly from those presented in Gladwin and others (1991), owing to a refinement of the selection of data windows since that time. The dominant signals present are the coseismic strain offsets of the Loma Prieta earthquake. These have been documented elsewhere (Gladwin and others, 1991); the present discussion is confined to the observed strain-rate changes. In figure 2*B* the coseismic offsets have been removed from the data to make long term trends more apparent.

It is important to investigate how choices made in estimating and removing the exponential borehole response can influence interpretation of the strain data determined from the gauge residuals. These effects are examined in figure 3. The representative strain data shown are produced from residuals obtained for three different data windows marked a, b and c used in the fitting procedure. We are documenting an apparent change of strain rate at the time of the Loma Prieta earthquake. The critical issue is whether the choice of data interval significantly affects determination of the strain-rate change. It is evident from figure 2 that any reasonable choice of fitted window demonstrates that a gradient change occurred in the raw datasets. For the extremes of fitting intervals shown, the effect on the observed change of strain rate before and after the Loma Prieta earthquake are shown in table 1.

Interval c is inappropriate because it extends into the data which is to be used to determine the pre-earthquake gradient. In the following discussion, interval b has been used because it gave the best variance over the available 1987 dataset.

RESULTS

An anomalous change in γ_1 is apparent by late 1988, showing a remarkably linear strain accumulation of 1 $\mu\varepsilon$ per year relative to the pre-1988 rate (Gladwin and others, 1991). The azimuth of maximum shear for the accumulating shear strain is approximately parallel to the local San Andreas fault strike. The long-term stability of the measurements is particularly evident in the areal strain data. Areal strain is estimated from the sum of the three components and is seen to be constant (with the exception of the coseismic offset at the Loma Prieta event) at better than 1 microstrain over the whole 10-year period.

Immediately after the earthquake the fault-parallel shear-strain rate decreased for about 2 months and then gradually returned to the pre-anomaly value. These data are shown in figure 4. In May 1990, following the Chittenden aftershock sequence (four magnitude 4 to 5 earthquakes on April 18, 1990, centered on an area approximately 15 km north west of SJT), the present linear γ_1 shear accumulation rate of approximately 2 $\mu\varepsilon$ per year with the original sense had been established.

The absolute strain rates may of course differ from those indicated on these figures (approximately 1 $\mu\varepsilon$ per year from late 1988 to the Loma Prieta event, and approximately 2 $\mu\varepsilon$ per year relative to the pre-1988 rate from May 1990 through December 1993) because the data have been effectively detrended by the exponential removal procedure. The point at issue is that there are significant changes of strain rate documented in the data, one preceding the Loma Prieta earthquake and another following it. Both appear to be linear with time, and their relative magnitudes are not an artifact of the exponential removal procedure.

An alternative and useful means for determining the physical significance of these data is to plot γ_1 against γ_2 (see fig. 5). The shear state at a particular time is represented by a point in this shear space, its history is represented by the locus of these points, and the shear required to move from one shear state to another is the vector

➤ Figure 1.—*A*, Raw gauge data for the SJT site beginning 3 months after installation. Fitted exponential curves are shown offset for clarity. The recording system was nonoperational for 5 months during 1987. *B*, Residual gauge data produced by removal of the fitted exponentials. Units are nominal microstrain only.

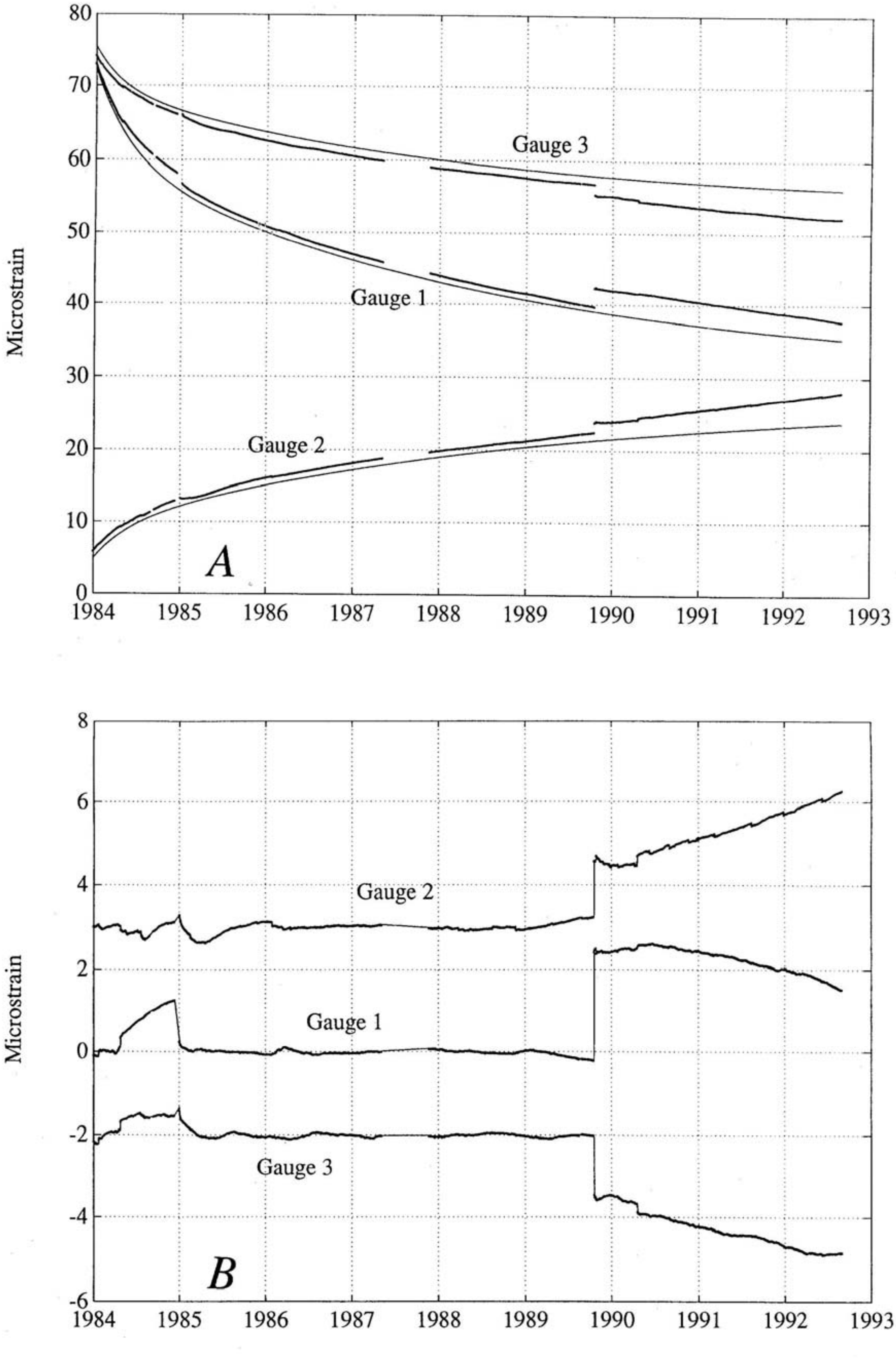
80
70
60
50
40
30
20
10
0
Microstrain
Gauge 3
Gauge 1
Gauge 2
A
1984
1985
1986
1987
1988
1989
1990
1991
1992
1993
8
6
4
2
0
-2
-4
-6
Microstrain
Gauge 2
Gauge 1
Gauge 3
B

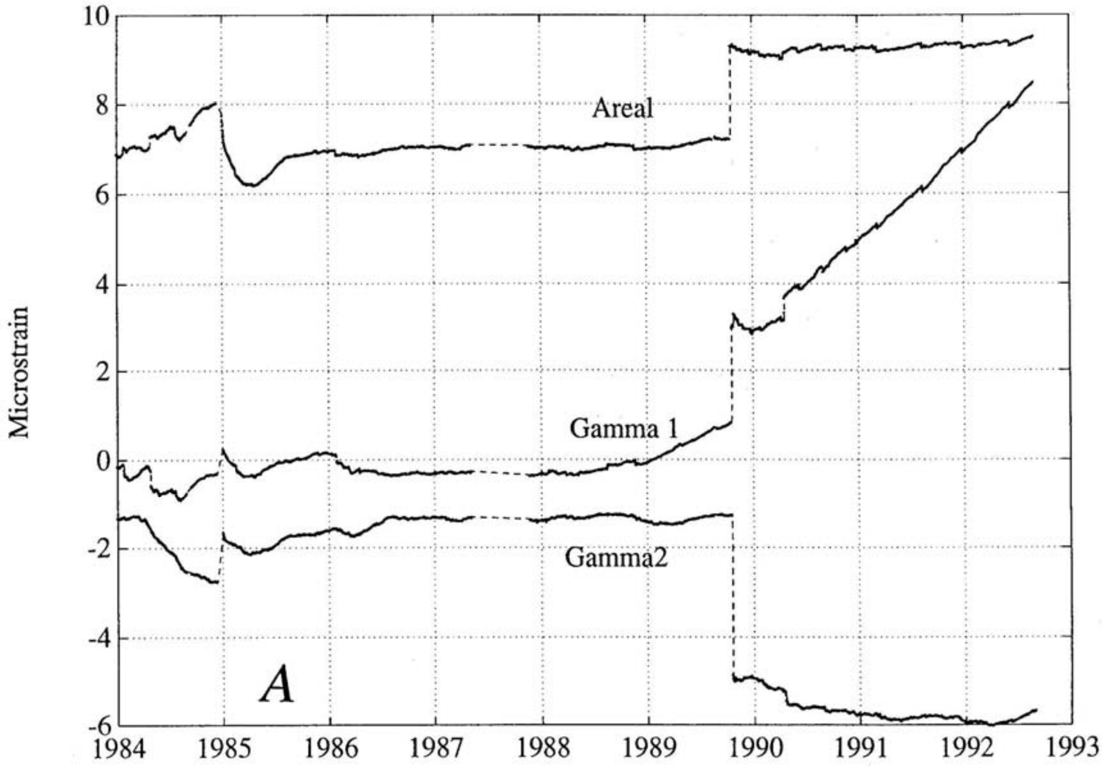
Microstrain
10
8
6
4
2
0
-2
-4
-6
1984
1985
1986
1987
1988
1989
1990
1991
1992
1993
Areal
Gamma 1
Gamma2
A

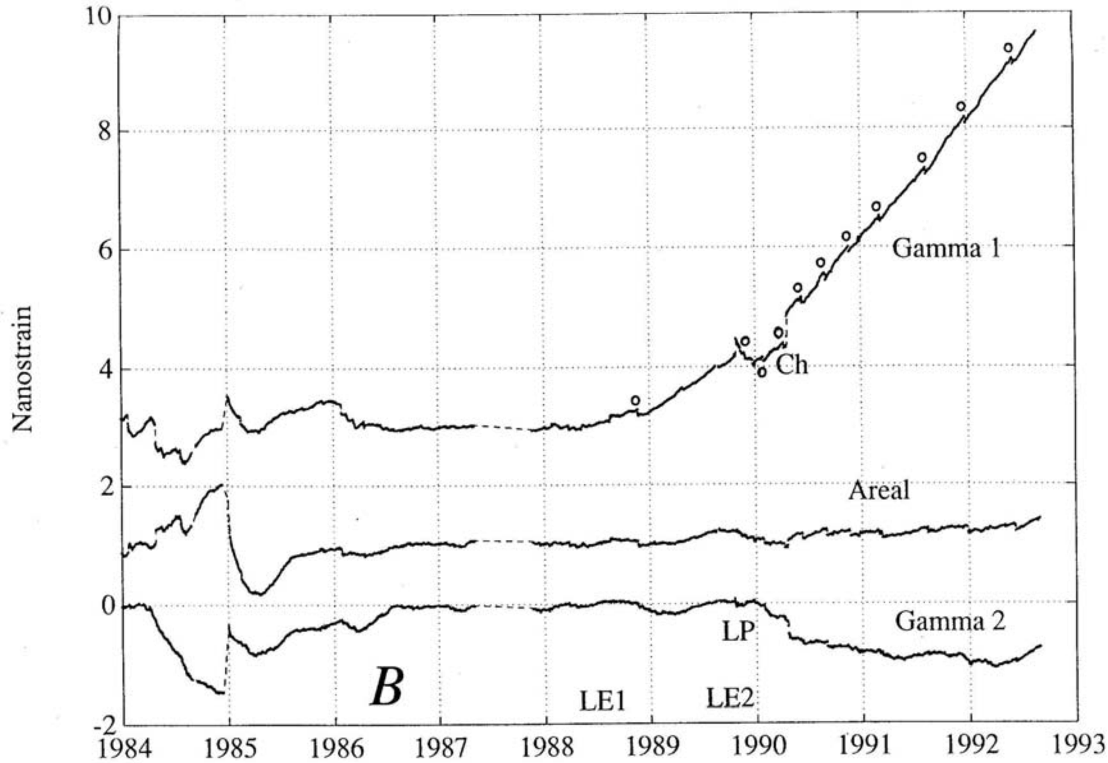
Nanostrain
10
8
6
4
2
0
-2
1984
1985
1986
1987
1988
1989
1990
1991
1992
1993
Gamma 1
Ch
Areal
Gamma 2
LP
B
LE1
LE2

connecting these points. With the local trace of the San Andreas approximately at N48°W, the γ_1 axis also represents approximately fault-parallel shear, and the γ_2 axis approximate extension normal to the fault. Time is marked at 3-month intervals, and direction of the coseismic offset of the Loma Prieta event is indicated in the upper and lower parts of the figure by the arrow. The Chittenden aftershock sequence is marked as CH on the lower part of the figure.

The shear-strain step C-C′, coseismic with the Loma Prieta event, is seen to increase both right-lateral shear across the fault (arising mainly from the γ_1 component, +1840 $n\varepsilon$) and normal compression (arising mainly from the γ_2 component, -3790 $n\varepsilon$). This fault-normal compression from shear alone must be combined with the contribution due to the areal strain step (+2140 $n\varepsilon$) to find the effective change in fault normal strain in the vicinity of the instrument of approximately 1600 $n\varepsilon$. Apart from a 5-month period immediately prior to the Loma Prieta event (see B-C in the figure) during which the maximum shear accumulation was oriented at N56°W, the predominant trend of both anomalies (see sections A-B and D-E in the figure) is a shear vector at angle E6°S corresponding to a maximum shear accumulation at N42°W, close to the local San Andreas fault strike of N48°W.

To verify instrument and coupling stability, response to earth strain tides was examined using the dominant, thermally uncontaminated tidal components O_1 and M_2. Sixty-day data windows of 90-minute data were used to provide normalised tidal component amplitude every 30 days. The strain step of the Loma Prieta event and other easily identifiable strain steps associated with earthquakes or creep events were removed from the record before the tidal analysis. Results are shown in figure 6 for the ε_a and γ_1 data sets. Error bars indicate the precision of determination for each point, assuming equal partition of noise over all tidal components. It is clear that there have been no significant or systematic changes of tidal admittance on this instrument over the whole period under discussion. This result has been confirmed elsewhere (Linde and others, 1991).

◄ Figure 2.—*A*, Areal strain and shear strains from the SJT borehole tensor strainmeter at San Juan Bautista near the San Andreas fault in northern California. Exponential trends have been removed from this data. A dominant feature is the coseismic strain step from the Loma Prieta earthquake in October 1989. *B*, Removal of this step reveals the details of the strain records, in particular the striking anomaly in the γ_1 component, the relative constancy of the other two strain components, and trend reversal on γ_1 for 3 months following the Loma Prieta event. All steps in the data can be associated with seismic events or nearby creep events. For example, the times of the two Lake Elsman earthquakes are indicated (LE1, LE2), as are the times of the Loma Prieta earthquake (LP), the Chittenden earthquake sequence (Ch), and creep events also monitored on a nearby creepmeter (o) and documented in table 2.

DISCUSSION

Apart from coseismic steps, the strain data show several readily identifiable steps which correlate closely with the main creep events on the closest creepmeter XSJ, 2 km to the east of our instrument. Events from late 1988 to 1992 are tabulated in table 2, and the detailed correspondence of the events with the main creep events gives further confidence that the data represent regional tectonic activity. Further, the events show (Gladwin and others, 1993) remarkable similarity suggestive of a small source (less than 0.5 kilometers in depth and at most a few kilometers in extent) directly under San Juan Bautista. The shear strain resulting from such a source cannot account for the size of the post Loma Prieta strain anomaly. Other explanations for this anomaly need to be examined.

A non-tectonic source from the instrument or its immediate vicinity is unlikely because of the stability of the tidal response, consistency of our internal instrument checks, the long-term stability of the areal strain record (better than 1 $\mu\varepsilon$ over 10 years), and the detailed correspondence in time of all observed strain steps with either earthquakes or creep events on nearby creep meters.

Though the strain signals could arise from small-scale processes in a nearby section of the fault, observations of anomalous creep events at three sites up to 30 km away indicate a more extended source. Figure 7 shows long-term creepmeter data for 5 sites covering 40 km of the fault south of San Juan Bautista with long-term trends (Burford, 1988). A distinct increase in creep rate following the Loma Prieta earthquake is evident on sites XSJ, XHR and CWC, spanning 16 km of the fault. The XFL site (29 km from XSJ) shows only a marginal increase, and the more remote site XMR (40 km) shows no effect.

The creep anomalies in figure 6 are unusual, especially for CWC and XHR, and begin at the time of the Loma Prieta earthquake. The creep anomaly at the nearby XSJ begins about the time of the establishment of the new shear strain anomaly at SJT, which, given the causal time correspondence, suggests that these signals are not just the consequence of normal interactions between fault sections in this creeping section, but are linked to the earthquake. We conclude that the failure of the Loma Prieta source region transferred load to the San Juan Bautista region just to its south, resulting in increased creep rate. The simplest explanation of an increased creep rate is frictional response to the increased fault-parallel shear loading indicated by the coseismic γ_1 step at San Juan Bautista.

However, slip via creep does not itself result in linearly increasing elastic strain. We suggest that our linear shear-strain anomaly is best explained by continued aseismic slip around a nearby locked section of the fault, the slip being associated with loading transferred from the Loma Prieta source region particularly after the Chittenden aftershock sequence (April 1990).

The response at the site immediately after the Loma Prieta earthquake and prior to the Chittenden events seems to indicate that this load transfer towards the SJT site was

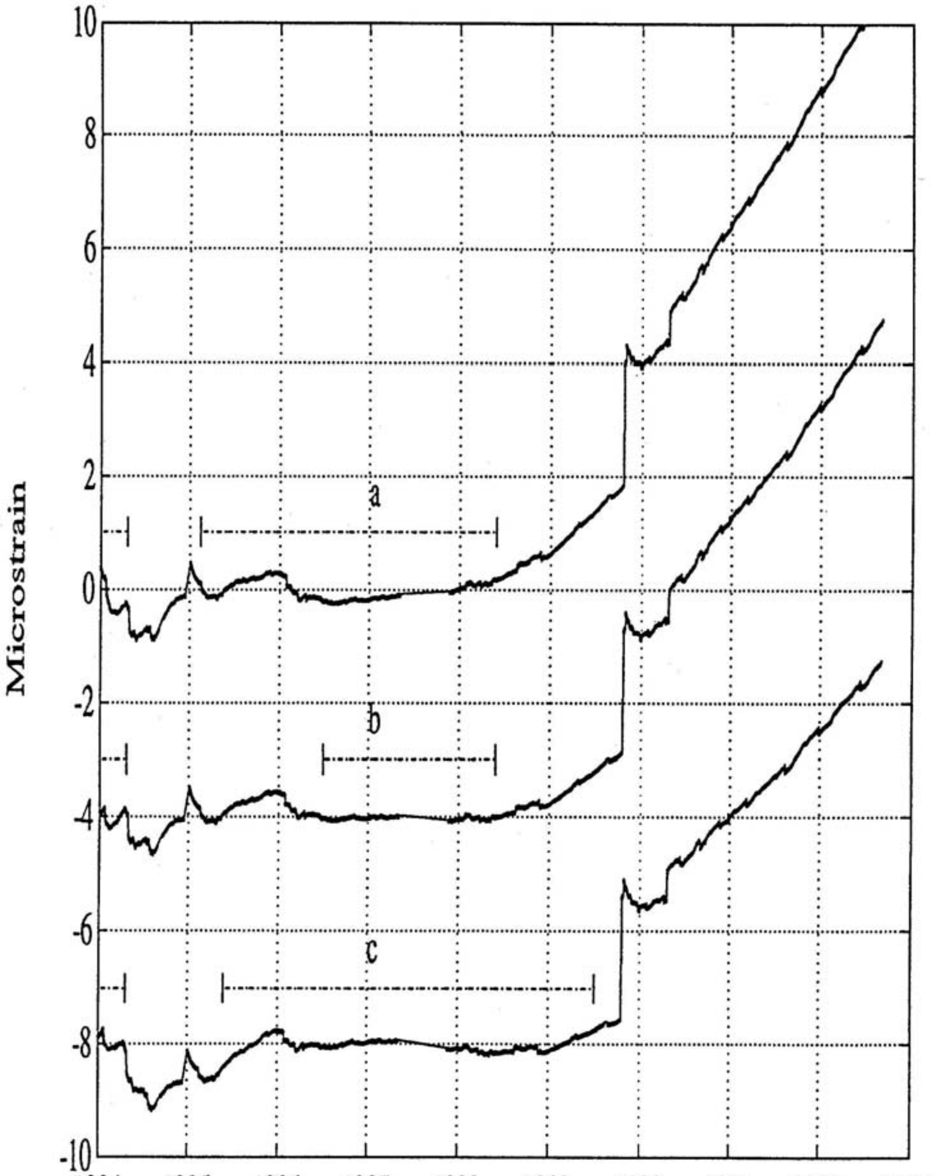

Figure 3.—Representative γ_l shear-strain data illustrating the effect of the choice of data window used for the exponential fitting. The intervals used in three separate fit sets are marked as a, b, and c. Estimates of the change of strain rate from before to after the Loma Prieta event are only marginally affected for the three extreme choices shown. The choices have some effect on the timing of the pre-event anomaly only. Note that for choice c the change of gradient is well defined before the end of the fitting interval, indicating that the end point of the fit interval is not producing the effects discussed. The changes of gradient that determine the anomalies under discussion are clear on all residual sets.

Table 1.—*Average gradient of shear strain γ_1 determined over three periods*

[Values are residual gauge data after removal of exponential functions fitted over the three selection intervals 1985/02 to 1988/04 (a), 1986/06 to 1988/04 (b), and 1985/05 to 1989/07 (c). The lowest row of data indicates that the change in strain rate after the Loma Prieta earthquake is very similar for the three fitting intervals shown.]

	Selection Interval		
	1985/02 to 1988/04 (a)	1986/06 to 1988/04 (b)	1985/05 to 1989/07 (c)
1986-1988	0.11 ± .11	-0.03 ± .08	0.01 ± .14
1989 to L.P.	1.56 ± .08	1.16 ± .09	0.75 ± .09
Post-L.P.	2.4 ± .10	2.01 ± .11	1.54 ± .12
Difference	0.84 ± .13	0.85 ± .14	0.79 ± .15

initially prevented by the strength of an asperity region associated with the Chittenden aftershock sequence. When this region ultimately failed in 1990, the SJT site immediately began to respond to the fault parallel shear expected from the Loma Prieta event in the sense of a continued afterslip at the Loma Prieta region.

A range of simple dislocation models of slip around a locked region were considered. The model which resulted in a fault-parallel shear-strain rate most comparable to that observed was a locked region extending along the fault strike at depth of 1.5 to 5 km, with the surrounding fault surface slipping at the regional average of 14 mm per year. While this model indicated a locked region shallower than the study mentioned above, uncertainty in the absolute value of the observed γ_2 strain rate indicates that our data are broadly consistent with the presence of such a locked region at moderate depth on the fault. The data thus suggest an increased probability of a moderate earthquake in the San Juan Bautista region.

We have previously suggested (Gladwin and others, 1991) that the pre-Loma Prieta strain changes were related to a broad regional effect, based on the timing of the Lake Elsman foreshock and a marginal geodetic anomaly (Lisowski and others, 1990) near the Loma Prieta source. The effects we are reporting also appear to have some regional expression in increased creep activity since the Loma Prieta earthquake. The anomaly in γ_1 is now so large that it would be expected to be detectable by geodetic observations in the area. Unfortunately, the major geodetic network is centered well to the north of San Juan Bautista, making even inversion for the determination of the southern extent of the Loma Prieta rupture zone itself difficult (Johnston and others, 1990). Recent data from the southern end of this network is not yet available, but a change of fault-parallel shear-strain rate of $1 \mu\varepsilon$ per year coincident with the Loma Prieta event should easily be identified in the observational period to date if it extended over the total geodetic network involved. These data are critical in providing constraints on the scaling of the anomaly in the northerly direction. Some data has been taken in a small HP3808 network extending from San Juan Bautista north to Pajaro Gap, particularly following the earthquake (Johnston, oral comm., 1993), but the results from this network are not yet published. Data from this network was not taken for many years prior to the Loma Prieta earthquake, so there is no likely contribution on the issue of whether or not a change of gradient has occurred following the event. There is no associated areal strain anomaly indicated in the data, and so no corroboration of the anomaly by reference to the dilatometer at Searle Road, approximately 5 km away, is available. The dilatometer shows no significant areal strain change.

Scaling of the anomaly cannot be determined from a single site, and the significance of these data will remain unknown until it is confirmed or denied from measurements at other nearby instrument sites. There is no evidence that the observed anomaly extends sufficiently far north to be measured in the Loma Prieta geodetic network. Our modelling suggests the presence of a source 5 km long. This source would produce minimal deformation in the geodetic network. Hence, although we are confident that the observed anomaly is not an instrumental artifact or of very localized origin, the only currently available supportive evidence that this anomaly is of regional significance is the increased creep activity in stations south of SJT.

ACKNOWLEDGMENTS

This work was performed under a grant from the U. S. Geological Survey, Department of the Interior. Contents do not represent policy of that agency, and no endorsement of the agency is to be assumed. The instruments were previously developed under awards of the Australian Research Grants Scheme and fabricated by R. Willoby and staff in-house. We thank R. Liechti for maintenance support, K. Breckenridge for data retrieval and assistance with creepmeter data, and Drs. A. Linde and M. Johnston for general support in the program.

REFERENCES CITED

Berry, D.S., 1967, Deformation of a circular hole driven through a stressed viscoelastic material: International Journal of Rock Mechanics and Mining Science, v. 4, p.181-187.

Berry, D.S., and Fairhurst, C., 1966, Influence of rock anisotropy and time-dependent deformation on the stress-relief and high-modulus inclusion techniques of in-situ stress determination: American Society for Testing Materials, STP 402, p.190-206.

Burford, R.O., 1988, Retardations in fault creep rates before local moderate earthquakes along the San Andreas fault system, central

California: Pure and Applied Geophysics, v. 126, p. 499-529.

Gladwin, M.T., 1984, High precision multi component borehole deformation monitoring: Reviews of Scientific Instruments, v. 55, p. 2011-2016.

Gladwin M.T., Breckenridge, K.S., Hart, R. and Gwyther, R.L., 1994, Measurements of the strain field associated with episodic creep events on the San Andreas Fault at San Juan Bautista, California: Journal of Geophysical Research, v. 99, no. B3, p. 4559-4565.

Gladwin, M.T., Gwyther, R.L., Hart, R. and Francis, M., 1987, Borehole tensor strain measurements in California: Journal of Geophysical Research, v. 92 , no. B8, p. 7981-7988.

Gladwin, M.T., Gwyther, R.L., Higbie, J.W. and Hart, R., 1991, A medium term precursor to the Loma Prieta earthquake?: Geophysical Research Letters, v. 18, no. 8, p. 1377-1380.

Gladwin, M.T., and Hart, R., 1985, Design parameters for borehole strain instrumentation. Pure and Applied Geophysics, v. 123, p. 59-88.

Gwyther, R.L., Gladwin, M.T., and Hart, R.H.G., 1992, A shear strain anomaly following the Loma Prieta earthquake: Nature, v. 356, p,142-144.

Jaeger, J.C. and Cook, N.G.W., 1967, Fundamentals of rock mechanics: London, Chapman and Hall.

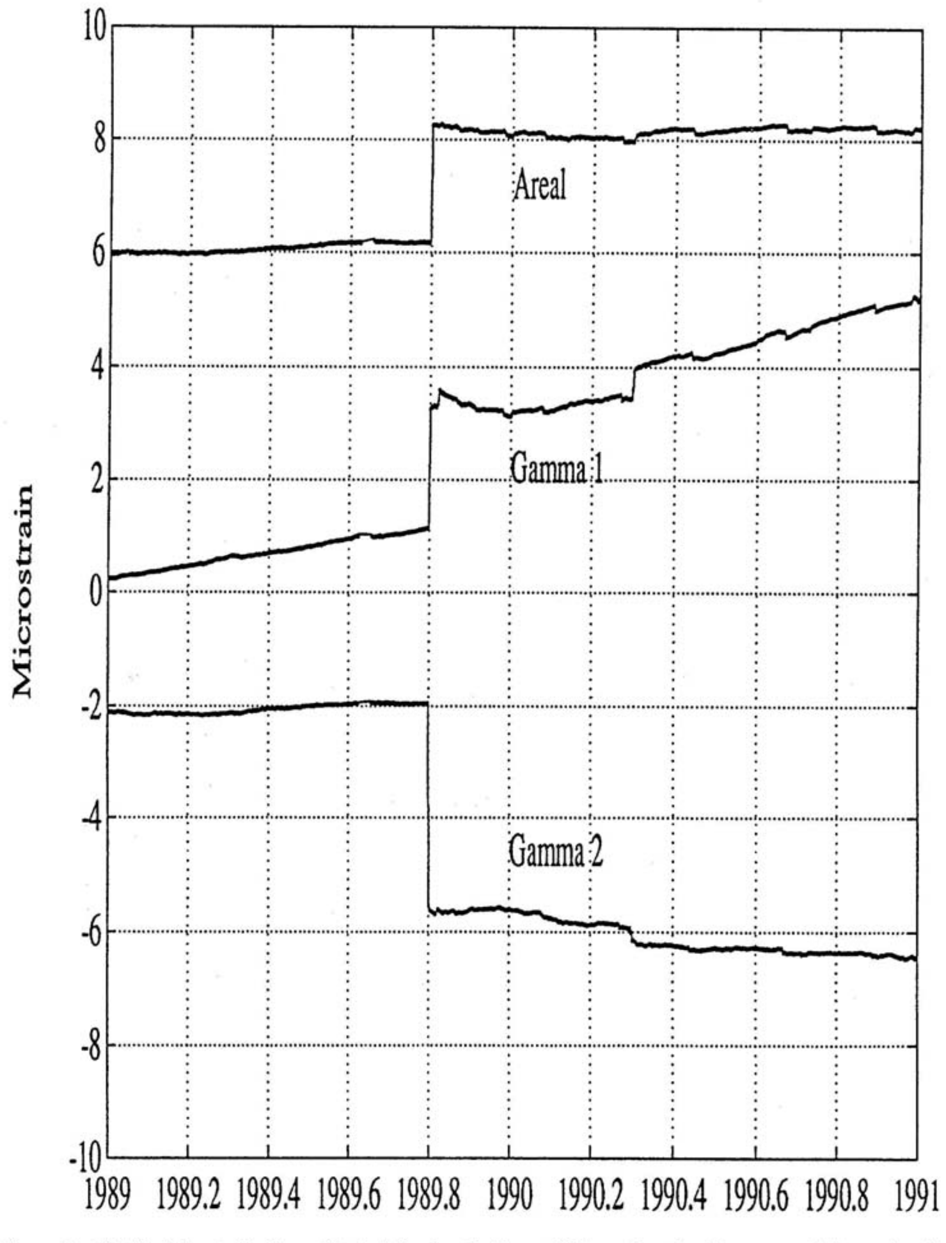

Figure 4.—Detail of the strains immediately following the Loma Prieta earthquake. The γ_l record shows that the post-earthquake strain rate shown in figure 2 did not begin until after the Chittenden sequence in April 1990.

Johnston, M.J.S., Linde, A.T., and Gladwin, M.T., 1990, Near-field high resolution strain measurements prior to the October 18, 1989, Loma Prieta Ms 7.1 earthquake: Geophysical Research Letters, v. 17, no. 10, p. 1777 - 1780.

Linde, A.T., Gladwin, M.T., and Johnston, M.J.S., 1991, The Loma Prieta earthquake, 1989 and earth strain tidal amplitudes: an unsuccessful search for associated changes: Geophysical Research Letters , v. 19 no. 3, p 317-320.

Lisowski, M., Prescott, W.H., Savage, J.C., and Svarc, J.L., 1990, A possible geodetic anomaly observed prior to the Loma Prieta, California, earthquake: Geophysical Research Letters, v. 17, no. 8, p. 1211-1214.

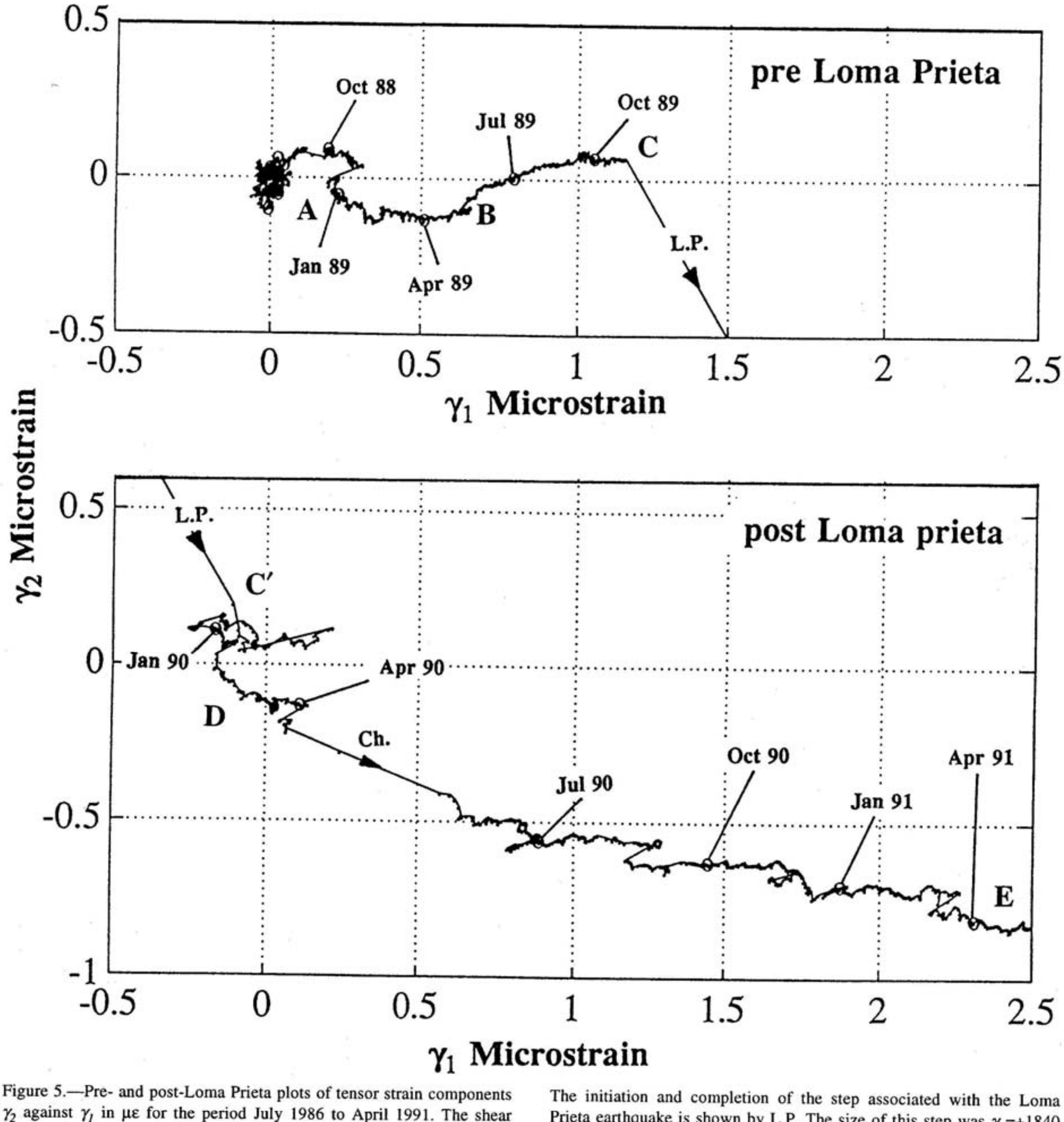

Figure 5.—Pre- and post-Loma Prieta plots of tensor strain components γ_2 against γ_1 in $\mu\varepsilon$ for the period July 1986 to April 1991. The shear strain γ_1 is a measure of shear strain approximately parallel to the San Andreas fault at this locality, while γ_2 is a measure of shear strain in approximately a north-south or east-west direction, and thus extension normal to the fault. Three monthly intervals are indicated on the figure. The initiation and completion of the step associated with the Loma Prieta earthquake is shown by L.P. The size of this step was γ_1=+1840 $n\varepsilon$ and γ_2=-3790 $n\varepsilon$. The Chittenden aftershock sequence strain step is indicated by Ch. For any shear-strain change ($\Delta\gamma_1$, $\Delta\gamma_2$), the maximum shear strain change is $\Delta\gamma = \sqrt{\Delta\gamma_1^2 + \Delta\gamma_2^2}$ and $\Theta = \frac{1}{2}\tan^{-1}[\Delta\gamma_2/\Delta\gamma_1]$ is the angle N of E for the axis of maximum extension.

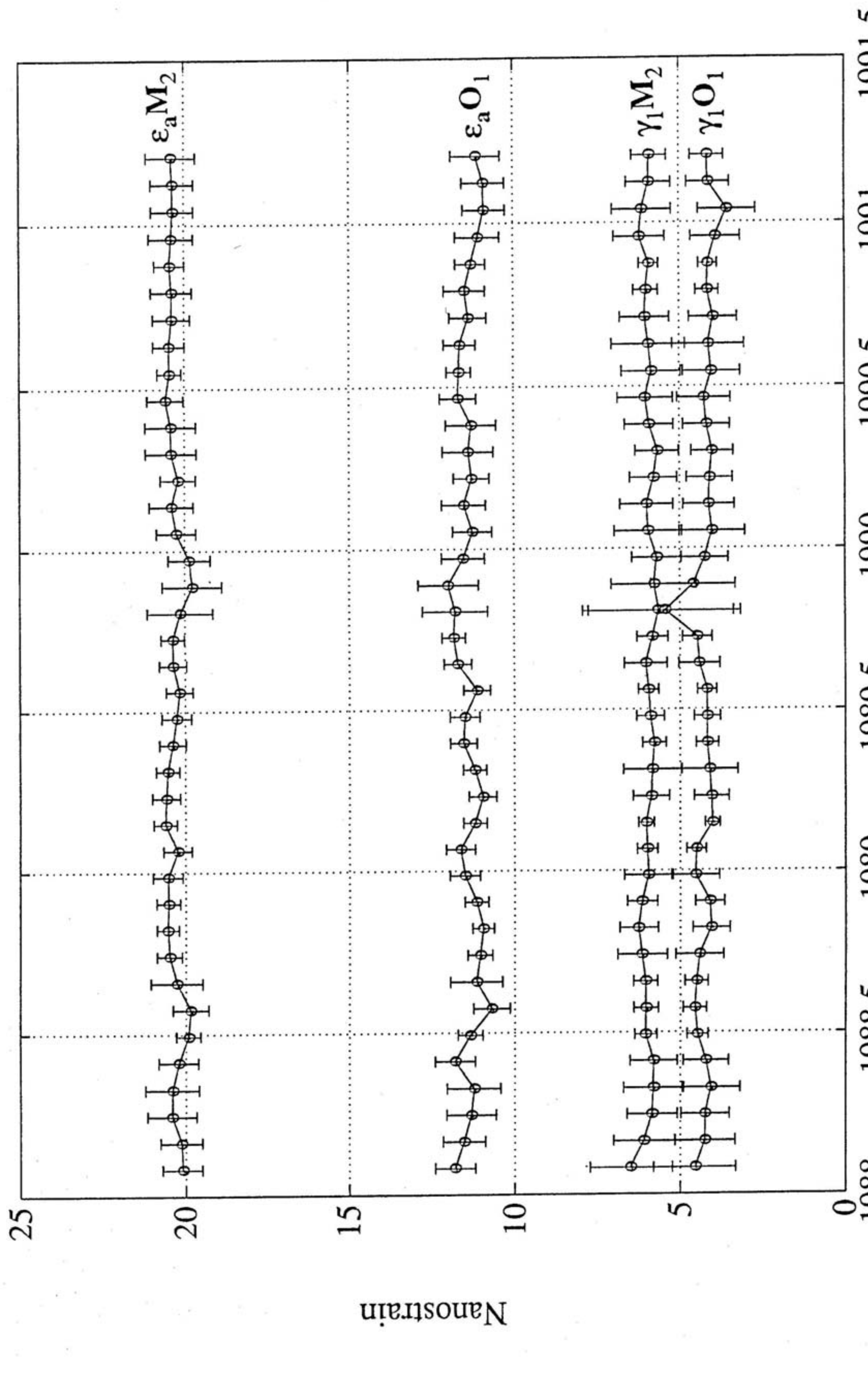

Figure 6.—Amplitude of the M_2 and O_1 tidal components of areal strain ε_a, and shear strain γ_l for the period 1988 to mid-1991. Sixty-day windows of 90-minute data were used to provide normalised tidal component amplitude every 30 days. The strain step of the Loma Prieta event and other easily identifiable strain steps were removed from the record. Error bars indicate the precision of determination, assuming Gaussian noise. There is no significant change in instrument performance for any component.

Table 2.—*Surface creep events recorded at XSJ creepmeter at San Juan Bautista in 1988-1992 period, and corresponding strain offsets observed at SJT*

[Each strain event preceded the surface creep event by less than 1 hour]

No.	Date	Strain event			Creep event
		γ_1	γ_2	ε_a	Size
		$n\varepsilon$	$n\varepsilon$	$n\varepsilon$	mm
1	21.11.88	-100	-40	-80	1.7
2	22.12.89	-77	-38	-60	0.5
3	27.01.90	-69	-41	-53	0.6
4	07.04.90	-90	-55	-75	1.9
5	09.06.90	-100	-50	-90	3.9
6	04.07.90		None		0.3
7	30.08.90	-120	-52	-91	3.2
8	20.11.90	-50	-45	-70	2.1
9	08.03.91	-95	-50	-80	3.6
10	06.08.91	-120	-50	-90	5.0
11	27.12.91	-90	-50	-80	0.3
12	07.06.92	-110	-45	-90	5.3

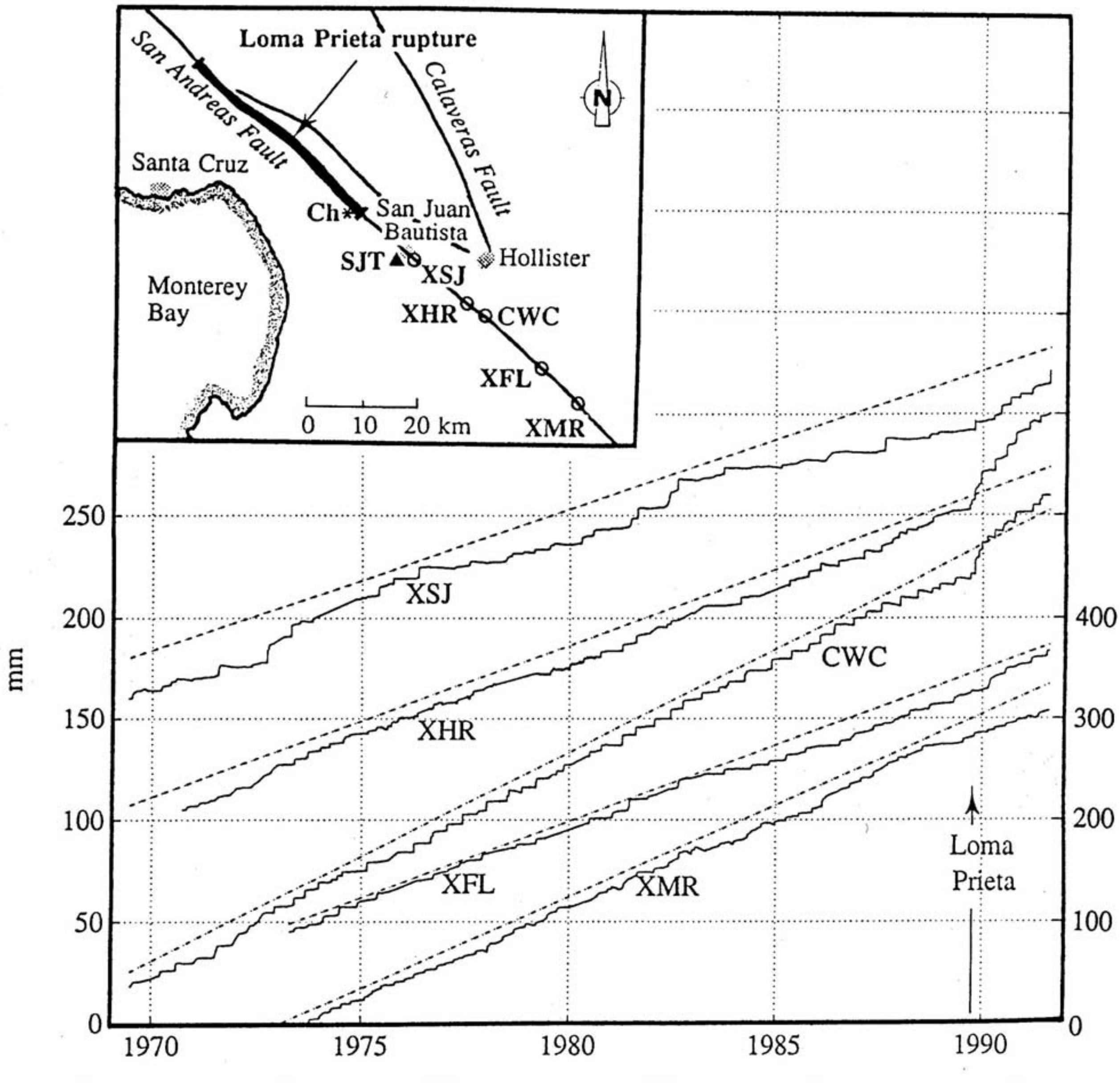

Figure 7.—Surface-creep data (provided by K. Breckenridge, USGS) from creepmeters along the fault south of San Juan Bautista, with positions of creepmeters XSJ, XHR, CWC, XFL and XMR, tensor strainmeter SJT, and Chittenden aftershock Ch indicated in the inset map. The trend lines indicated are from Burford (1988). Note that for the XMR data, the scale at the right axis should be used.